Hindawi

Research Article

Dynamic Behaviours and Bifurcation Analysis of a Filippov Ecosystem with Fear Effect

Ben Chu, Guangyao Tang ⓘ, and Changcheng Xiang ⓘ

School of Mathematics and Statistics, Hubei Minzu University, Enshi, Hubei 445000, China

Correspondence should be addressed to Guangyao Tang; tgy0201227@163.com and Changcheng Xiang; xcc7426681@126.com

Evidences of the fear effect of the prey are well documented, which can greatly affect the dynamics of the predator-prey system. In this study, considering that the fear effect of the prey is triggered on as the density of the predator reaches and exceeds a threshold value, we develop a Filippov system of predator-prey model with the fear effect. In addition, we also include a modify factor of the growth rate of the prey when they adopt the antipredator behaviours due to the fear effect. We initially analyze the dynamics of the two subsystems, including the existence and stability of the equilibria. Utilizing the theory of the Filippov system, we discuss the sliding dynamics, i.e., the existence of sliding region and sliding equilibria. By choosing the threshold as the bifurcation parameter, we investigate the bifurcations near the regular equilibria. The solution curve has three cases: crossing the threshold curve, sliding on the threshold curve, and approaching the pseudoequilibrium. Finally, we numerically verified the existence of the global sliding bifurcation near the regular equilibrium and also the touching bifurcation.

1. Introduction

Traditionally, the researchers usually connect the predator and their prey only through direct predations [1, 2]. In the recent decades, lots of experiments show that the relationship between the predator and the prey is far more complex than hunting. For one aspect, due to the fear effect of the predation [3–5], the prey will choose to adopt the antipredator behaviours, such as moving to new habitats, searching for safer foods, and other physiological changes, aiming at avoiding the predation. This will definitely help to decrease the death rate of the prey. However, the growth rate of the preys will also be decreased because of the extra costs of adopting antipredator behaviours. Therefore, there could be the trade-off of the fear effect on the growth of the prey. Also, it will be important to study the impacts of the fear effect of prey on the dynamic behaviours between the prey and their predators.

Recently, some scholars have also considered the influence of fear effect on the dynamic behaviours of predator-prey models. For example, Wang et al. [6] first proposed a predator-prey model with the fear effect. In their paper,

they have demonstrated a correlation between the fear effect and the direct effect of predators on prey and gave three specific expressions for the fear effect. They also demonstrated that the fear effect does not affect the dynamic behaviours of the system with the Holling-I response function. However, when the functional response is Holling-II, higher levels of fear can stabilize the system by eliminating the presence of oscillatory behaviours. When the appropriate birth rate and fear effect are selected, the system will have a limit cycle. The authors in [7] established a Beddington–DeAngelis predator-prey model with fear effect, refuge, and harvest. They found that there is a critical value of the fear effect, and the two species can continue to exist for a long time through positive density levels. There are also other critical values so that both species can exist at a positive density, but their density levels swing periodically over time. Zhang et al. [8] proved that the system exhibits multiple spatiotemporal patterns due to spatial memory delay and nonlocal fear effect delay. Researchers explored the impact of the fear effect and the Leslie–Gower function on the dynamical behaviours of the predator-prey model and found that as the fear effect increases, the dynamical behaviours of

the system switches multiple times until the prey eventually becomes extinct, while the predator survives due to the presence of alternative prey in [9]. For more relevant research on the fear effect, refer to the literature [10–14].

When the number of predators reaches a certain level, the prey will have a fear effect and show antipredator behaviours, resulting in a change in the functional response between the predator and the prey. Therefore, we need to establish a model with threshold conditions. But most predator-prey models are described by ordinary differential equations with continuous right-hand sides, but these models cannot reflect the influence of refuge, group defense, and other factors on population dynamics. Therefore, a discontinuous right-hand nonsmooth dynamic system widely used in mechanics has attracted the attention of ecologists [15–19]. This kind of system is called the Filippov system or switched system, which provides a basic framework for the establishment of many mathematical models with practical significance [20–22]. Therefore, based on the above research, this study proposes a Filippov predator-prey model, which depends on the number of predators using the threshold strategy. Our model extends the existing predator-prey model with the fear effect by introducing a threshold strategy to describe the impact of the fear effect when the number of predators exceeds the threshold. When the number of predators is below the threshold, the functional response is Holling-I. When the number of predators is above the threshold, the functional response changes to Holling-II, and the fear effect is produced.

This study is organized as follows: In Section 2, a Filippov predator-prey model with fear effect is established, and the basic theory and related definitions of the Filippov system will be provided. In Section 3, the dynamic behaviours of the two subsystems are analyzed. In Section 4, the sliding region, sliding dynamics, and the existence of various equilibria of the model are analyzed theoretically. In Section 5, the regular/virtual equilibrium bifurcation, boundary equilibrium bifurcation, and global sliding bifurcation are numerically verified. Finally, the conclusions are presented in Section 6.

2. Model Formulation and Preliminaries

2.1. Model Formulation. We use the classical Lotka–Volterra model to describe the interaction between the predator and prey [23], i.e.,

$$
\begin{cases}
\dfrac{dx}{dt} = rx - dx - ax^2 - pxy, \\[2mm]
\dfrac{dy}{dt} = upxy - my,
\end{cases}
\tag{1}
$$

where x and y represent the population density of prey and predator, respectively. In model (1), the growth of prey follows the logistic mode, and predator-prey interactions follow the Holling-I functional response. r and d are the natural birth rate and natural mortality rate of the prey, respectively, a indicates the decay rate of the prey due to

intraspecific competition, and p denotes the rate of search for the prey by the predator. The rate of conversion of prey biomass to predator biomass is denoted by u, and m expresses the natural mortality of the predator. In addition, the assumption that $r > d$ will apply to the entire article.

We assume that the fear effect of the prey to their predator is triggered on by a threshold value of the density of predators Y_T. That is, there is no fear effect before the predator reaches the threshold value Y_T, and the interactions between the predator and prey is assumed to follow model (1). When $y > Y_T$, due to the fear effect, the prey may adopt the antipredator behaviours, such as moving to new habitats or searching for safer foods and other physiological changes, aiming at avoiding the predation; consequently, there should be a limitation of the predation of the predator to the prey. Hence, we use the Holling-II response function as the existence of fear effects of the prey. In addition, the antipredator behaviours will also lead to the extra costs of the prey, reflecting on the decreasing of its growth rate. Also, we use the factor to modify the growth rate of prey due to the antipredator behaviours induced by the fear effect. Then, the predator-prey model with the fear effect becomes [6]

$$
\begin{cases}
\dfrac{dx}{dt} = \phi(k, y)rx - dx - ax^2 - \dfrac{pxy}{1 + qx}, \\[2mm]
\dfrac{dy}{dt} = \dfrac{upxy}{1 + qx} - my,
\end{cases}
\tag{2}
$$

where q is the half-saturation constant and $\phi(k, y)$ is a decreasing function with respect to k and y. k reflects the degree of fear that drives antipredatory behaviours in prey. According to the biological significance of k, y, and $\phi(k, y)$, the function $\phi(k, y)$ should satisfy the following four assumptions:

(1) $\phi(0, y) = 1$: if there is no fear, there will be no impact on prey. In other words, the natural birth rate of the prey population will not decrease

(2) $\phi(k, 0) = 1$: if there are no predators, there is no fear effect on prey, and therefore the natural birth rate of prey does not decrease

(3) $(\partial\phi(k, y)/\partial k) < 0$: the natural birth rate of prey decreases with the increasing fear effect

(4) $(\partial\phi(k, y)/\partial y) < 0$: if the density of predators increases, the fear effect increases, and therefore the natural birth rate of prey decreases

A simple form of $\phi(k, y)$ with the above assumptions satisfied is $\phi(k, y) = 1/1 + ky$, proposed by [6]. So, system (2) can be rewritten as follows:

$$
\begin{cases}
\dfrac{dx}{dt} = \dfrac{rx}{1 + ky} - dx - ax^2 - \dfrac{pxy}{1 + qx}, \\[2mm]
\dfrac{dy}{dt} = \dfrac{upxy}{1 + qx} - my.
\end{cases}
\tag{3}
$$

So, systems (2) and (3) can be integrated into the following nonsmooth dynamical system:

$$\begin{cases} \dfrac{dx}{dt} = \dfrac{rx}{1 + \varepsilon ky} - dx - ax^2 - \dfrac{pxy}{1 + \varepsilon qx}, \\[3mm] \dfrac{dy}{dt} = \dfrac{upxy}{1 + \varepsilon qx} - my, \end{cases} \tag{4}$$

with

$$\varepsilon = \begin{cases} 0, & y < Y_T, \\ 1, & y > Y_T. \end{cases} \tag{5}$$

2.2. Preliminaries. To further analyze the Filippov system, here are some symbols [24–26]. Let $R_+^2 = \{Z = (x, y)^T \mid x \geq 0, y \geq 0\}$, $F_{S_i}: R_+^2 \longrightarrow R_+^2$, $(i = 1, 2)$ be the smooth vector fields and ε be a partition function that depends on $y - Y_T$. Let $H(Z) = y - Y_T$ be a smooth scalar function with a nonzero gradient whose threshold value depends on the number of individuals in the predator. Thus, (5) can be rewritten as given in the following equation:

$$\varepsilon = \begin{cases} 0, & H(Z) < 0, \\ 1, & H(Z) > 0. \end{cases} \tag{6}$$

For convenience, we denote

$$F_{S_1} = \left(rx - dx - ax^2 - pxy, upxy - my\right)^T,$$

$$F_{S_2} = \left(\dfrac{rx}{1 + ky} - dx - ax^2 - \dfrac{pxy}{1 + qx}, \dfrac{upxy}{1 + qx} - my\right)^T. \tag{7}$$

Then, system (4) with (6) can be rewritten as the following Filippov system:

$$\dot{Z}(t) = \begin{cases} F_{S_1}(Z), & Z \in S_1, \\ F_{S_2}(Z), & Z \in S_2, \end{cases} \tag{8}$$

where $S_1 = \{Z \in R_+^2 \mid H(Z) < 0\}$ and $S_2 = \{Z \in R_+^2 \mid H(Z) > 0\}$. Σ be called as the switching manifold, which is the separation boundary of the region and the discontinuity boundary set Σ can be defined as

$$\Sigma = \left\{Z \in R_+^2 \mid H(Z) = 0\right\}. \tag{9}$$

Furthermore, Σ divides R_+^2 into two distinct regions S_1 and S_2. Then, the Filippov system (8) in region S_i is called subsystem S_i, $i = 1, 2$.

Let

$$\begin{aligned} \sigma(Z) &= \langle H_Z(Z), F_{S_1}(Z)\rangle \cdot \langle H_Z(Z), F_{S_2}(Z)\rangle \\ &= F_{S_1}H(Z) \cdot F_{S_2}H(Z), \end{aligned} \tag{10}$$

where $\langle \cdot \rangle$ denotes the standard scalar product, and Lie derivative $F_{S_i}H(Z) = \langle H_Z(Z), F_{S_i}(Z)\rangle \,(i = 1, 2)$ is used to denote the directional derivative of H concerning the vector field $F_{S_i}\,(i = 1, 2)$ at Z. Therefore, we partition the discontinuity boundary according to the sign case of $\sigma(Z)$.

Accordingly, the boundary will be classified as follows:

(i) $\Sigma_e \in \Sigma$ is called the escaping region if $F_{S_1}H(Z) < 0$ and $F_{S_2}H(Z) > 0$ on Σ_e

(ii) $\Sigma_s \in \Sigma$ is called the sliding region if $F_{S_1}H(Z) > 0$ and $F_{S_2}H(Z) < 0$ on Σ_s

(iii) $\Sigma_c \in \Sigma$ is called the crossing region if $F_{S_1}H(Z) \cdot F_{S_2}H(Z) > 0$ on Σ_c

For the convenience of the later study, it is useful to list the definitions of the various equilibria of the Filippov system [16, 17] for this paper.

Definition 1. If a point Z^* makes $F_{S_1}(Z^*) = 0, H(Z^*) < 0$ or $F_{S_2}(Z^*) = 0, H(Z^*) > 0$, the point Z^* is called the regular equilibrium of the Filippov system (8). If a point Z^* makes $F_{S_1}(Z^*) = 0, H(Z^*) > 0$ or $F_{S_2}(Z^*) = 0, H(Z^*) < 0$, the point Z^* is called the virtual equilibrium of the Filippov system (8).

Definition 2. If a point Z^* is the equilibrium of the sliding region of the Filippov system (8), the point Z^* is called pseudoequilibrium and $Z^* \in \Sigma_s$, that is, $(1 - \lambda)F_{S_1}(Z^*) + \lambda F_{S_2}(Z^*) = 0, H(Z^*) = 0$, and $0 < \lambda < 1$, where

$$\lambda = \frac{\langle H_Z(Z), F_{S_1}(Z)\rangle}{\langle H_Z(Z), F_{S_1}(Z) - F_{S_2}(Z)\rangle}. \tag{11}$$

Definition 3. If $F_{S_1}(Z^*) = 0, H(Z^*) = 0$ or $F_{S_2}(Z^*) = 0, H(Z^*) = 0$, the point Z^* is called a boundary equilibrium of the Filippov system (8).

Definition 4. If $Z^* \in \Sigma_s$, $H(Z^*) = 0$, and $\langle H_Z(Z^*), F_{S_1}(Z^*)\rangle = 0$ or $\langle H_Z(Z^*), F_{S_2}(Z^*)\rangle = 0$, the point Z^* is called a tangent point of the Filippov system (8).

3. Dynamics Analysis of Subsystems

The Filippov system (8) consists of three parts: two smooth subsystems and a discontinuity boundary, so it is necessary to study the dynamical behaviours of two subsystems before analyzing the complete Filippov system. In this section, we analyze the existence and stability of the equilibria of the two subsystems separately.

3.1. Dynamics of the Subsystem S_1. When $y < Y_T$, the dynamical behaviours of system (8) is determined by the subsystems defined by (1). The subsystem S_1 has the following three equilibria: $E_{01} = (0, 0)$, $E_{11} = (r - d/a, 0)$, and $E_1^* = (x_1^*, y_1^*)$ where $x_1^* = m/up, y_1^* = (up(r - d) - ma)/(up^2)$. The equilibria E_{01} and E_{11} always exist. The point E_1^* is in the first quadrant if $r > d + (am/up)$. The following theorem will give the possible dynamical behaviours of all equilibria and the conditions under which they occur.

Theorem 5

(I) The trivial equilibrium $E_{01} = (0, 0)$ is a saddle

(II) The boundary equilibrium $E_{11} = (r - d/a, 0)$ is locally asymptotically stable if

$$r < d + \frac{am}{up}. \tag{12}$$

(III) The interior equilibrium $E_1^* = (x_1^*, y_1^*)$ is locally asymptotically stable when (12) is violated

Proof. We analyze the stability of the equilibria by analyzing the corresponding Jacobian matrix for each equilibrium. Now, the Jacobian matrix at $E_{01} = (0, 0)$, $E_{11} = (r - d/a, 0)$, and $E_1^* = (x_1^*, y_1^*)$ are given by

$$J_{E_{01}} = \begin{pmatrix} r - d & 0 \\ 0 & -m \end{pmatrix}, J_{E_{11}} = \begin{pmatrix} d - r & \dfrac{p(d - r)}{a} \\ 0 & \dfrac{up(r - d)}{a} - m \end{pmatrix}, \text{ and}$$

$$J_{E_1^*} = \begin{pmatrix} r - d - 2ax_1^* - py_1^* & -px_1^* \\ upy_1^* & upx_1^* - m \end{pmatrix}. \tag{13}$$

Since $tr(J_{E_{01}}) = r - d - m$ and $det(J_{E_{01}}) = -m(r - d) < 0$, the trivial equilibrium E_{01} is a saddle.

The trace and determinant corresponding to the matrix $J_{E_{11}}$ are $tr(J_{E_{11}}) = (up - a)(r - d)/a - m$ and $det(J_{E_{11}}) = (d - r)(up(r - d)/a - m)$. Both $tr(J_{E_{11}})$ and $det(J_{E_{11}})$ can be positive or negative, therefore, from the Routh–Hurwitz criterion, it follows that E_{11} is locally asymptotically stable when $tr(J_{E_{11}}) < 0$ and $det(J_{E_{11}}) > 0$. Thus, the boundary equilibrium is locally asymptotically stable when $r < d + (am/up)$. Similarly, the condition of local asymptotic stability of internal equilibrium E_1^* is $r > d + (am/up)$. $\square$

Theorem 6. *When $r \in (d, d + (am/up))$, the boundary equilibrium E_{11} is globally asymptotically stable. When $r \in (d + (am/up), +\infty)$, the interior equilibrium E_1^* is globally asymptotically stable.*

Proof. The two functions on the right-hand side of system (1) are denoted by $P(x, y)$ and $Q(x, y)$. We consider the Dulac function as $B(x, y) = 1/xy$. After calculations, we obtain

$$D = \frac{\partial(PB)}{\partial x} + \frac{\partial(QB)}{\partial y} = -\frac{a}{y} < 0. \tag{14}$$

For $(x, y) \in int(R_+^2) = (0, \infty) \times (0, \infty)$. Thus, according to the Dulac–Bendixson theorem, system (1) has no periodic orbits in $(0, \infty) \times (0, \infty)$. Besides, when $r > d + (am/up)$, the positive equilibrium in $(0, \infty) \times (0, \infty)$ has only the interior equilibrium E_1^*. So all positive solutions will tend to E_1^*. Combining the E_1^* proved in Theorem 5 is locally asymptotically stable, it can be concluded that E_1^* is globally asymptotically stable if condition (12) does not hold.

When $r \in (d, d + (am/up))$, there are only two equilibria E_{01} and E_{11} in R_+^2. In addition, there is no periodic orbit in R_+^2 which means that every positive solution converges to E_{01} or E_{11}. It is easy to obtain that E_{01} is repelling when $r > d$, so every positive solution converges to E_{11}. Combining the E_{11} proved in Theorem 5 is locally asymptotically stable, it can be concluded that E_{11} is globally asymptotically stable if $r \in (d, d + (am/up))$. $\square$

3.2. Dynamics of the Subsystem S_2. For the subsystem S_2, it is easy to calculate the following three equilibria: $E_{02} = (0, 0)$, $E_{12} = (r - d/a, 0)$ and $E_2^* = (x_2^*, y_2^*)$ where $x_2^* = m/up - mq$, $y_2^* = (-C_2 + \sqrt{C_2^2 - 4C_1 C_3})/(2C_1)$ with

$$C_1 = k(up - mq)^2, C_2 = (up - mq)^2$$
$$+ uk(am + du\, p - dm), \text{ and} \tag{15}$$
$$C_3 = u(am + (d - r)(up - mq)).$$

Notice that the equilibria E_{01} and E_{11} are always present and the equilibrium E_2^* is feasible if $r > d + (am)/(up - mq)$ with $up > mq$.

Theorem 7. *The trivial equilibrium $E_{02} = (0, 0)$ is a saddle.*

Proof. The Jacobian matrix at $E_{02} = (0, 0)$ is

$$J_{E_{02}} = \begin{pmatrix} r - d & 0 \\ 0 & -m \end{pmatrix}. \tag{16}$$

Obviously, we can get $tr(J_{E_{02}}) = r - d - m$ and $det(J_{E_{02}}) = -m(r - d) < 0$, so by the Routh–Hurwitz criterion it follows that the trivial equilibrium E_{02} is a saddle. $\square$

The following lemmas [6] give the stability analysis regarding the boundary equilibrium E_{02} and the internal equilibrium E_2^*.

Lemma 8. *The boundary equilibrium E_{02} is locally asymptotically stable if*

$$(r - d)(up - mq) < am, \tag{17}$$

is satisfied and is unstable if

$$(r - d)(up - mq) > am, \tag{18}$$

holds.

Lemma 9. *The boundary equilibrium E_{02} is globally asymptotically stable if $up \leq mq$ holds.*

Lemma 10. *The internal equilibrium E_2^* is locally asymptotically stable if*

$$\begin{cases} r > d + \dfrac{am}{up - mq}, \\[2mm] r \leq d + \dfrac{a(up + mq)}{q(up - mq)}, \\[2mm] up > mq, \end{cases} \tag{19}$$

or

$$
\begin{cases}
r > d + \dfrac{a(up + mq)}{q(up - mq)}, \\[4mm]
k > \dfrac{q(up - mq)^2 ((r - d)q(up - mq) - a(up + mq))}{u^2 pa(qd(up - mq) + a(up + mq))}, \\[4mm]
up > mq.
\end{cases}
\tag{20}
$$

It is unstable if

$$
\begin{cases}
r > d + \dfrac{a(up + mq)}{q(up - mq)}, \\[4mm]
k < \dfrac{q(up - mq)^2 ((r - d)q(up - mq) - a(up + mq))}{u^2 pa(qd(up - mq) + a(up + mq))}, \\[4mm]
up > mq.
\end{cases}
\tag{21}
$$

Lemma 11. *The internal equilibrium E_2^* is globally asymptotically stable if*

$$
\begin{cases}
r > d + \dfrac{am}{up - mq}, \\[4mm]
r \le d + \dfrac{a(up + mq)}{q(up - mq)}, \\[4mm]
up > mq, \\[3mm]
up - mq \le rq.
\end{cases}
\tag{22}
$$

4. Sliding Region and Equilibria of the Filippov System (8)

In this section, we calculate the sliding region and various equilibria of the Filippov system (8) according to the definitions.

4.1. Sliding Segment and Region. Through simple calculation, the following Lie derivatives can be obtained:

$$
F_{S_1} H(Z) = Y_T (upx - m),
\tag{23}
$$

$$
F_{S_1} H(Z) = Y_T \left(\frac{upx}{1 + qx} - m \right).
\tag{24}
$$

Let the right-hand sides of the above two functions be zero to get $x_{S_1} = m/up$ and $x_{S_2} = m/up - mq$. By definitions, we can obtain the following theorem for the sliding region, escaping region, and crossing region.

Theorem 12

(I) If $x_{S_2} > 0$, the sliding and crossing segment of the Filippov system (8) can be defined as

$$
\Sigma_s = \left\{ (x, y) \in \Sigma \mid x_{S_1} < x < x_{S_2} \right\},
$$

$$
\Sigma_c = \left\{ (x, y) \in \Sigma \mid 0 < x < x_{S_1} \right\} \cup \left\{ (x, y) \in \Sigma \mid x_{S_2} < x \right\}.
\tag{25}
$$

(II) If $x_{S_2} < 0$, the escaping and crossing segment of the Filippov system (8) can be defined as

$$
\Sigma_e = \left\{ (x, y) \in \Sigma \mid 0 < x < x_{S_1} \right\},
$$

$$
\Sigma_c = \left\{ (x, y) \in \Sigma \mid x_{S_1} < x \right\}.
\tag{26}
$$

Proof

(I) If $x_{S_2} > 0$, we can know that $0 < x_{S_1} < x_{S_2}$. According to (23), (24), and the definition of sliding region, we obtain the sliding region

$$
\Sigma_s = \left\{ (x, y) \in \Sigma \mid x_{S_1} < x < x_{S_2} \right\}.
\tag{27}
$$

Moreover, there are two possible scenarios that can lead to the presence of transversal intersection and crossing region:

$$
F_{S_1} H(Z) > 0 \text{ and } F_{S_2} H(Z) > 0,
\tag{28}
$$

or

$$
F_{S_1} H(Z) < 0 \text{ and } F_{S_2} H(Z) < 0.
\tag{29}
$$

From (28), we calculate that $x < x_{S_1}$ and $x < x_{S_2}$, i.e., $x < \min\{x_{S_1}, x_{S_2}\}$. So, we get the crossing region $\Sigma_{c1} = \left\{ (x, y) \in \Sigma \mid 0 < x < x_{S_1} \right\}$. Also, from (29), we can get $x > x_{S_1}$ and $x > x_{S_2}$, i.e., $x > \max\{x_{S_1}, x_{S_2}\}$. Thus, the crossing region is $\Sigma_{c2} = \left\{ (x, y) \in \Sigma \mid x_{S_2} < x \right\}$. In summary, the crossing region is

$$
\Sigma_c = \left\{ (x, y) \in \Sigma \mid 0 < x < x_{S_1} \right\} \cup \left\{ (x, y) \in \Sigma \mid x_{S_2} < x \right\}.
\tag{30}
$$

(II) If $x_{S_2} < 0$, we can know that $x_{S_2} < 0 < x_{S_1}$. By definition, we can get $x < x_{S_1}$ and $x > x_{S_2}$. Thus, the escaping region is

$$
\Sigma_e = \left\{ (x, y) \in \Sigma \mid 0 < x < x_{S_1} \right\}.
\tag{31}
$$

Similarly, (28) and (29) can be obtained for the crossing region. Simplifying (28) can yield $x < x_{S_1}$ and $x < x_{S_2}$, i.e., $x < \min\{x_{S_1}, x_{S_2}\}$. To ensure that the solution must satisfy

biological significance, x must be a non-negative constant, so this situation does not exist. For (29), the calculation gives $x > x_{S_1}$ and $x > x_{S_2}$, i.e., $x > \max\{x_{S_1}, x_{S_2}\}$. So the crossing region is

$$\Sigma_c = \left\{(x, y) \in \Sigma \mid x_{S_1} < x\right\}. \qquad (32)$$
□

We next examine the existence of four types of equilibria of the Filippov system (8) according to the definitions in Section 2.2.

4.2. Pseudoequilibrium. Based on Definition 2, we first calculate

$$\lambda = \frac{(upx - m)(qx + 1)}{pqux^2}. \qquad (33)$$

So,

$$1 - \lambda = \frac{(mq - up)x + m}{pqux^2}. \qquad (34)$$

Substituting the expressions for λ and $1 - \lambda$ into $(1 - \lambda)F_{S_1}(Z^*) + \lambda F_{S_2}(Z^*) = 0$, we can obtain the following equation:

$$\begin{cases} \dfrac{dx}{dt} = \dfrac{C_4 x^3 + C_5 x^2 + C_6 x + C_7}{pqux(1 + kY_T)}, \\[3mm] \dfrac{dy}{dt} = 0, \end{cases} \qquad (35)$$

where $C_4 = -apqu(1 + kY_T)$, $C_5 = -pqu(d(1 + kY_T) - r)$, $C_6 = -(mpqY_T(1 + kY_T) + krY_T(up - mq))$, and $C_7 = kmrY_T$.

We know from [27] that we only need to discuss the case of the molecular roots of (dx/dt).

Let

$$F(x) = C_4 x^3 + C_5 x^2 + C_6 x + C_7. \qquad (36)$$

It can be seen that the intersection of the function with the vertical axis is $A = (0, C_7)$ $(C_7 > 0)$. Its derivative is

$$F'(x) = 3C_4 x^2 + 2C_5 x + C_6. \qquad (37)$$

From this, it follows that the discriminant of the roots of the derivative equation and the axis of symmetry of the image are

$$\Delta = 4C_5^2 - 12C_4 C_6, \quad X = -\frac{C_5}{3C_4} > 0. \qquad (38)$$

Since all parameters are non-negative numbers, C_4 is less than zero and C_7 is large than zero. From the uniform persistence of the system it follows that $r/1 + kY_T - d > 0$, therefore C_5 is large than zero. However, the sign of C_6 can be positive or negative.

The next step is to determine the positive roots of the original function based on the derivative.

(A) C_6 is a non-negative number

In this case, $\Delta > 0$ and the intersection of $F'(x)$ with the vertical axis is $B = (0, C_6)$ $(C_6 \geqslant 0)$. It follows that $F(x)$ monotone increasing and then decreasing on $(0, +\infty)$. $F(x)$ intersects with the positive half axis of the longitudinal axis, so $F(x)$ has one positive root. This solution is the horizontal coordinate of the pseudoequilibrium, denoted by x_1^p. So the coordinates of the pseudoequilibrium is $E_1^p = (x_1^p, Y_T)$. See Figure 1(a).

(B) C_6 is a negative number

In this case, the sign of Δ can be positive or negative. Therefore, we will discuss these categories.

  (I) $\Delta \leq 0$
  In this case, since $C_4 < 0$ and $\Delta \leq 0$, $F'(x) \leq 0$. It follows that $F(x)$ is monotone decreasing on $(0, +\infty)$ and because $F(x)$ intersects the positive semiaxis of the vertical axis, $F(x)$ has one positive root. This solution is the horizontal coordinate of the pseudoequilibrium, denoted by x_2^p. So the coordinate of the pseudoequilibrium is $E_2^p = (x_2^p, Y_T)$. See Figure 1(b).

  (II) $\Delta > 0$
  Combining all the above conditions shows that $F'(x)$ has two distinct positive roots. Suppose the two roots are x_- and x_+ $(x_- < x_+)$. Therefore, $F(x)$ is monotone decreasing, then monotone increasing, and finally monotone decreasing on $(0, +\infty)$. There are five possible scenarios for the solution of $F(x)$ as follows:

  (i) When $F(x_-) > 0$, $F(x)$ has one positive root. Therefore, the solution is the horizontal coordinate of the pseudoequilibrium, denoted by x_3^p. So the coordinate of the pseudoequilibrium is $E_3^p = (x_3^p, Y_T)$. See Figure 1(c).

  (ii) When $F(x_-) = 0$, $F(x)$ has two positive roots, one of which is x_- and the other is set to x_5^p. Hence the coordinates of the pseudoequilibria are $E_4^p = (x_-, Y_T)$ and $E_5^p = (x_5^p, Y_T)$. Beyond that, we know that $x_- < x_5$. See Figure 1(d).

  (iii) When $F(x_-) < 0$ and $F(x_+) > 0$, $F(x)$ has three positive roots. Let these three positive roots be x_6^p, x_7^p and x_8^p. Therefore, the coordinates of the pseudoequilibria are $E_6^p = (x_6^p, Y_T)$, $E_7^p = (x_7^p, Y_T)$ and $E_8^p = (x_8^p, Y_T)$. Furthermore, we assume that $x_6 < x_7 < x_8$. See Figure 1(e).

  (iv) If $F(x_-) < 0$ and $F(x_+) = 0$, then $F(x)$ has two positive roots. One of the roots is x_+ and the other root is set to x_9^p. In addition, we know that $x_9 < x_+$. Therefore, the coordinates of the pseudoequilibria are $E_9^p = (x_9^p, Y_T)$ and $E_{10}^p = (x_+, Y_T)$. See Figure 1(f).

  (v) If $F(x_-) < 0$ and $F(x_+) < 0$, then $F(x)$ has one positive root. Therefore, the solution is the horizontal coordinate of the pseudoequilibrium, denoted by x_{11}^p. So the coordinate of the
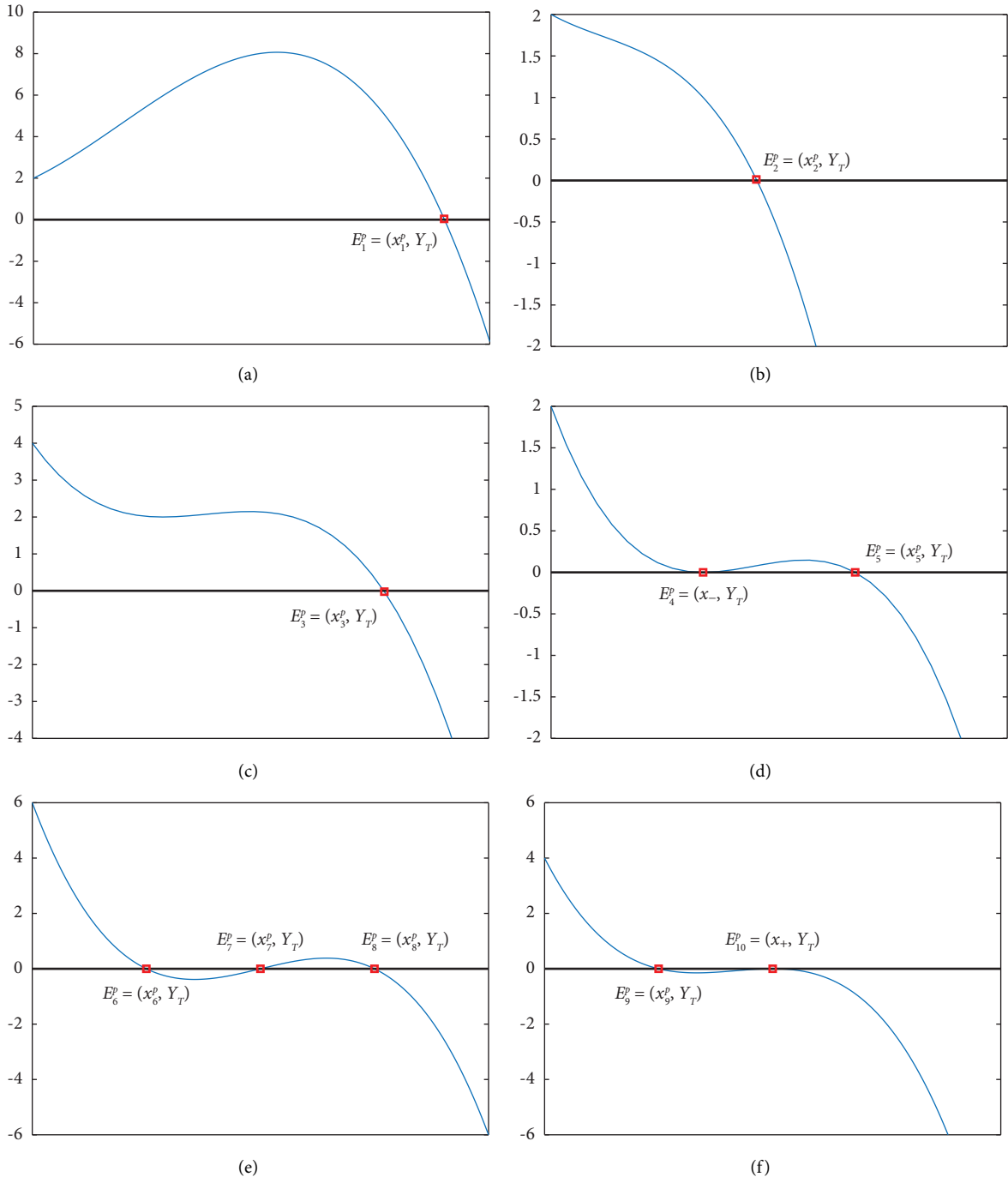
(a)

(b)

(c)

(d)

(e)

(f)

Figure 1: Continued.

(g)

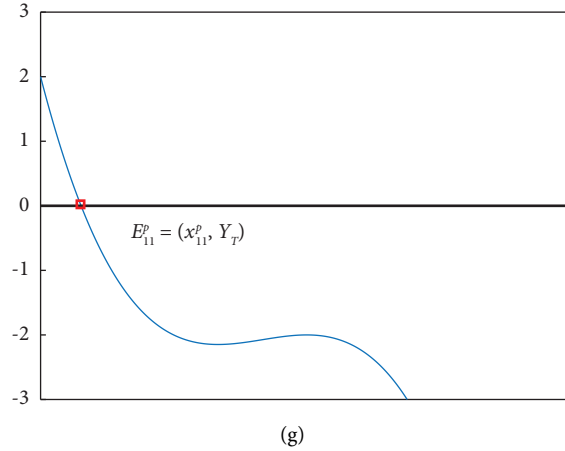FIGURE 1: Possible shapes of the graph of $F(x) = C_4 x^3 + C_5 x^2 + C_6 x + C_7$, where (a) is for $C_6 \geq 0$, (b) is for $C_6 < 0$ and $\Delta \leq 0$, and (c–g) are for $C_6 < 0$ and $\Delta > 0$.

pseudoequilibrium is $E_{11}^P = (x_{11}^P, Y_T)$. See Figure 1(g).

Next, we analyze the stability of the pseudoequilibria. We can see from Figure 1 that $F'(x) < 0$ when $x = x_i^P$ ($i = 1, 2, 3, 5, 6, 8, 9, 11$), so the pseudoequilibrium E_i^P is stable. $F'(x) > 0$ when $x = x_7^P$, so the pseudoequilibrium E_7^P is unstable. By using the proof of Theorem 5 in [28] it can be shown that E_{10}^P is a stable pseudoequilibrium and E_4^P is an unstable pseudoequilibrium.

We summarize the above in Table 1.

4.3. Regular Equilibria.
For the subsystem S_1, $E_{01} = (0, 0)$, and $E_{11} = (r - d/a, 0)$ are regular equilibria. Furthermore, for the equilibrium $E_1^* = (x_1^*, y_1^*)$ there are the following conclusions. Before discussing whether E_1^* is a regular or virtual equilibrium, it is necessary to ensure that it exists, in

other words, to ensure that the condition $r > d + (am/up)$ holds. If $y_1^* < Y_T$, then the equilibrium E_1^* is a regular equilibrium for the subsystem S_1, denoted by E_1^R. If $y_1^* > Y_T$, then the equilibrium E_1^* is a virtual equilibrium, denoted by E_1^V.

Moreover, about regular equilibria for the subsystem S_2, $E_{02} = (0, 0)$, and $E_{12} = (r - d/a, 0)$ are virtual equilibria. In addition, we have the following results based on the size of Y_T and y_2^*. If $y_2^* > Y_T$ and $r > d + (am)/(up - mq)$ with $up > mq$, then the equilibrium E_2^* is a regular equilibrium for the subsystem S_2, denoted by E_2^R. If $y_2^* > Y_T$ and $r > d + (am)/(up - mq)$ with $up > mq$, then the equilibrium E_2^* is a virtual equilibrium for the subsystem S_2, denoted by E_2^V.

The expressions of y_1^* and y_2^* are complex, so their sizes cannot be directly compared. First, we assume that $y_1^* > y_2^*$. Then, we obtain an inequality between the parameter k and the other parameters

$$k > \frac{u^3 p^4 ((r - d)(up - mq) - ma) - up^2 (up - mq)^2}{(up - mq)^2 (up(r - d) - ma)^2 + u^2 p^2 (am + d(up - mq))} = k^*. \tag{39}$$

Similarly, when assuming that $y_1^* < y_2^*$ it is obtained that $k < k^*$.

Based on the above analysis, when both E_1^* and E_2^* exist and $k > k^*$, if $y_2^* < Y_T < y_1^*$, then the equilibria E_1^* and E_2^* are virtual equilibria. However, when both E_1^* and E_2^* exist and $k < k^*$, if $y_1^* < Y_T < y_2^*$, then both E_1^* and E_2^* are regular equilibria.

We summarize the regular and virtual states of the internal equilibria under different conditions in the following Table 2.

4.4. Boundary Equilibrium.
The boundary equilibrium of the Filippov system (8) satisfies the following equation:

$$\begin{cases} \dfrac{rx}{1 + \varepsilon k y} - dx - ax^2 - \dfrac{pxy}{1 + \varepsilon q x} = 0, \\\\ \dfrac{upxy}{1 + \varepsilon q x} - my = 0, \\\\ y = Y_T. \end{cases} \tag{40}$$

We denote E_1^B provided (40) as $\varepsilon = 0$, i.e., $Y_T = y_1^*$ (if y_1^* exists) and E_2^B provided (40) as $\varepsilon = 1$, i.e., $Y_T = y_2^*$ (if y_2^* exists).

So, the coordinates of the boundary equilibria are given in the following equation:

TABLE 1: Summary of pseudoequilibrium.

Condition	The case of pseudoequilibrium
$C_6 \geq 0$	E_1^P (stable)
$C_6 < 0$ and $\Delta \leq 0$	E_2^P (stable)
$C_6 < 0$, $\Delta > 0$, and $F(x_-) > 0$	E_3^P (stable)
$C_6 < 0$, $\Delta > 0$, and $F(x_-) = 0$	E_4^P (unstable) and E_5^P (stable)
$C_6 < 0$, $\Delta > 0$, $F(x_-) < 0$, and $F(x_+) > 0$	E_6^P (stable), E_7^P (unstable), and E_8^P (stable)
$C_6 < 0$, $\Delta > 0$, $F(x_-) < 0$, and $F(x_+) = 0$	E_9^P (stable) and E_{10}^P (unstable)
$C_6 < 0$, $\Delta > 0$, $F(x_-) < 0$, and $F(x_+) < 0$	E_{11}^P (stable)

TABLE 2: Summary of regular equilibria.

Prerequisite	Size relation between Y_T and y_i^* ($i = 1, 2$)	Regular and virtual state of equilibria
$k > k^*$	$y_2^* > Y_T$	E_1^V, E_2^R
	$y_2^* < Y_T < y_1^*$	E_1^V, E_2^V
	$y_1^* < Y_T$	E_1^R, E_2^V
$k < k^*$	$y_1^* > Y_T$	E_1^V, E_2^R
	$y_1^* < Y_T < y_2^*$	E_1^R, E_2^R
	$y_2^* < Y_T$	E_1^R, E_2^V

$$E_1^B = \left(\frac{m}{up}, Y_T\right), Y_T = y_1^* = \frac{up(r-d) - ma}{up^2},$$

$$E_2^B = \left(\frac{m}{up - mq}, Y_T\right), Y_T = y_2^* = \frac{-C_2 + \sqrt{C_2^2 - 4C_1C_3}}{2C_1}.$$

(41)

Therefore, the boundary equilibria E_1^B and E_2^B exist at the critical values y_1^* and y_2^* of Y_T, respectively.

4.5. Tangent Points. According to Definition 4, a point $E_T = (x_T, Y_T)$ will be a tangent point on sliding segment Σ_s if

$$F_{S_1}H(Z) = 0 \text{ or } F_{S_2}H(Z) = 0. \quad (42)$$

Accordingly, the following equations are obtained:

$$upxy - my = 0, \quad (43)$$

or

$$\frac{upxy}{1 + qx} - my = 0. \quad (44)$$

The coordinates of the two tangent points can be obtained by solving the above equations (43) and (44): $E_1^T = (m/up, Y_T)$ and $E_2^T = (m/up - mq, Y_T)$. When Y_T is the critical value y_1^* (y_2^*), the boundary equilibria E_1^B (E_2^B) collide with the tangent points E_1^T (E_2^T).

5. Sliding Bifurcation Analysis of the Filippov System (8)

5.1. Regular/Virtual Equilibrium Bifurcation. Based on the above analysis of the different equilibria it is known that r and Y_T are the key factors that determine the existence of different types of equilibria. Therefore, we define four curves with respect to the parameters r and Y_T as follows:

$$L_1 = \left\{(r, Y_T) \mid r = d + \frac{am}{up}\right\},$$

$$L_2 = \left\{(r, Y_T) \mid r = d + \frac{am}{up - mq}\right\},$$

$$L_3 = \left\{(r, Y_T) \mid Y_T = \frac{up(r-d) - ma}{up^2}\right\}, \quad (45)$$

$$L_4 = \left\{(r, Y_T) \mid Y_T = \frac{-C_2 + \sqrt{C_2^2 - 4C_1C_3}}{2C_1}\right\},$$

where C_1, C_2, and C_3 have the same expressions as in (15).

The four curves divide the parameter space into seven regions and mark whether the equilibrium in each region is regular equilibrium or virtual equilibrium. Similarly, the boundary equilibria E_1^B and E_2^B appear on the corresponding curves L_3 and L_4. In particular, in Figure 2, not only the two virtual equilibria E_1^V and E_2^V can coexist, but also the two regular equilibria E_1^R and E_2^R. Therefore, when other parameters are fixed, the regular and virtual states of the internal equilibria of different thresholds will be different according to the size of the birth rate, and the number threshold of prey's fear effect on predators will affect the future development trend of the prey population.

5.2. Boundary Equilibrium Bifurcation. Boundary equilibrium bifurcation may occur in the Filippov system (8) once E_P, E_T, and E_R or E_T and E_R collide at the same time as Y_T passes a critical value, where E_P, E_T, and E_R represent the pseudoequilibrium, tangent point, and regular equilibria of the system, respectively. In this part, Y_T is chosen as the bifurcation parameter, and all other parameters are fixed as those in Figures 3 and 4.

5.2.1. Boundary Node Bifurcation. A simple calculation gives the critical value of Y_{T1} of 0.2864. When $Y_T = 0.1$, the stable node E_2^R exists. Also, the visible tangent point E_2^T exists on the boundary, as shown in Figure 3(a). It can be seen from the Figure 3(a) that the trajectories starting from region S_2 and remaining at S_2 without colliding with the boundary will converge to E_2^R. The trajectories from region S_2 will also collide with the sliding region or the crossing region. The trajectories which hit the sliding region will pass through the visible tangent point E_2^T and finally converge to E_2^R. At the same time, the trajectories of collision with the crossing
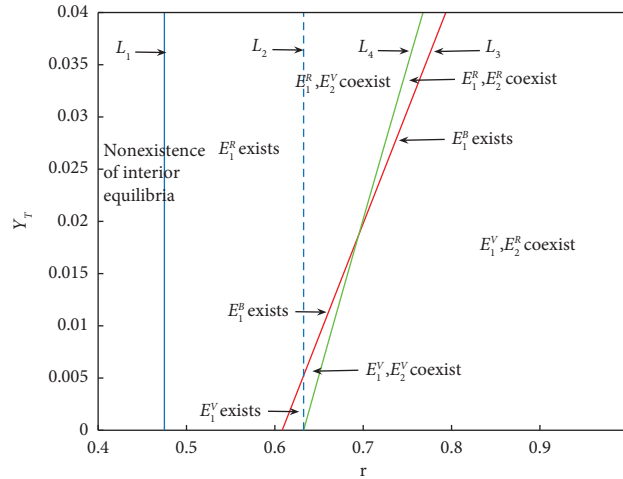
FIGURE 2: Regular/virtual equilibrium. The parameter values are fixed as follows: $a = 1$, $m = 0.1$, $u = 0.8$, $p = 0.6$, $d = 0.4$, $q = 0.5$, and $k = 6$.

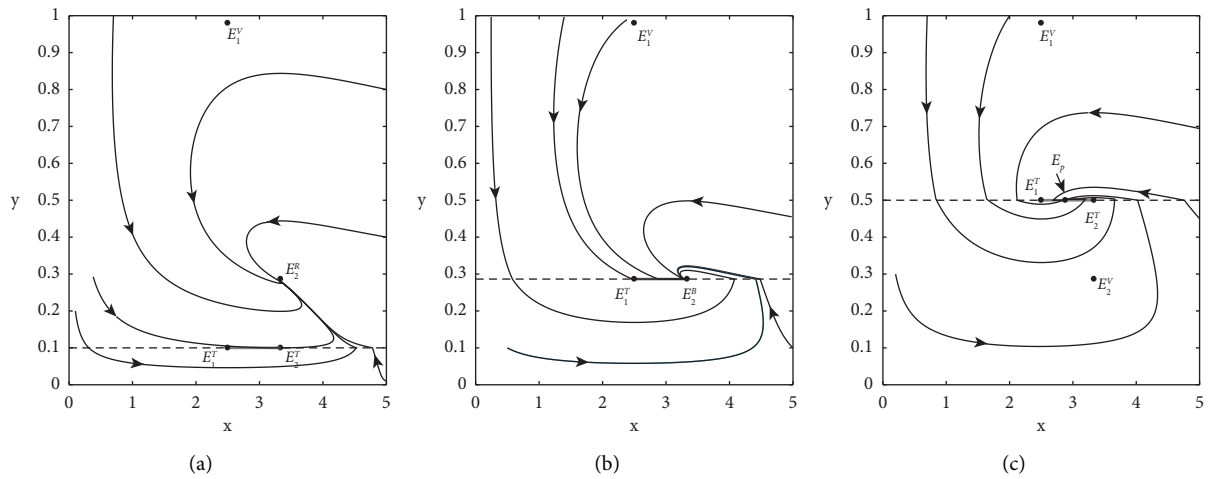(a)   (b)   (c)

FIGURE 3: Boundary node bifurcation for system (8). Here, we choose Y_T as a bifurcation parameter and fix all other parameters as follows: $r = 1$, $k = 1$, $d = 0.01$, $a = 0.2$, $p = 0.5$, $q = 0.1$, $u = 0.4$, $m = 0.5$, and (a) $Y_T = 0.1$; (b) $Y_T = 0.2864$; (c) $Y_T = 0.5$.

region converges to E_2^R. The trajectories from region S_1 will cross the crossing region and eventually converge to E_2^R.

The regular equilibrium E_2^R becomes boundary equilibrium E_2^B which collides with the tangent point E_2^T, when $Y_T = 0.2864$. All the trajectories hitting sliding region or crossing region will converge to E_2^B, see Figure 3(b) for more details.

For $Y_T = 0.5$, the regular equilibrium E_2^R will turn into a virtual equilibrium E_2^V. At the same time, the visible tangent point E_2^T becomes the invisible tangent point E_2^T. In addition, the pseudoequilibrium E_P also exists. In this case, the trajectories will remain on the sliding segment and converge to pseudoequilibrium E_P, as shown in Figure 3(c).

5.2.2. Boundary Focus Bifurcation. The critical value Y_{T2} is 0.98. From Figure 4(a), the stable focus E_1^R and the virtual equilibrium E_2^V coexist when $Y_T = 1.2$. The visible tangent point E_1^T exist. In this case, the trajectories will converge to the regular equilibrium E_1^R.

For $Y_T = 0.98$, the stable focus E_1^R becomes boundary equilibrium E_1^B which collides with the tangent point E_1^T. In this case, all the trajectories hitting discontinuous boundary will converge to E_1^B, see Figure 4(b) for more details.

The boundary equilibrium E_1^B will turn into the virtual equilibrium E_1^V, and the visible tangent point E_1^T becomes invisible tangent point E_1^T. In this case, the trajectories will converge to the pseudoequilibrium E_P, as shown in Figure 4(c).

5.3. Global Sliding Bifurcation. It can be seen from [6] that there may be standard periodic solutions that lie entirely in the region S_2 when the subsystem S_2 through a Hopf bifurcation. At the same time, as described in [29], the Filippov system (8) may add a new periodic solution that slides in the sliding segment, that is, the sliding periodic solutions. The orbits corresponding to the sliding cycle solutions are called sliding cycles. In this section, we focus on grazing bifurcation (i.e., touching bifurcation).
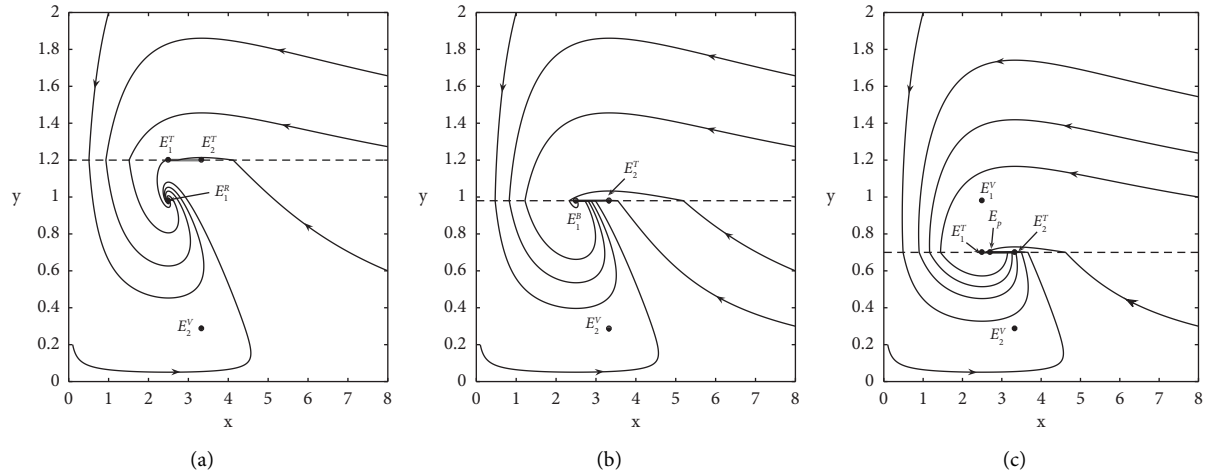
(a)   (b)   (c)

FIGURE 4: Boundary focus bifurcation for system (8). Here, we choose Y_T as a bifurcation parameter, (a) $Y_T = 1.2$; (b) $Y_T = 0.98$; and (c) $Y_T = 0.7$, where other parameters are given in Figure 3.

It is known from [29] that standard periodic solutions can collide with sliding segments, and this bifurcation is called a grazing (touching) bifurcation. When $Y_T = 6$, the region S_2 of the Filippov system (8) will have a stable periodic solution, see Figure 5(a) for more details. At this point, there are two tangent points E_1^T and E_2^T lying on the sliding boundary. The subsystem S_2 has an unstable regular equilibrium E_2^R and subsystem S_1 has an unstable virtual equilibrium E_1^V. It can be seen from Figure 5(b) that when the threshold Y_T increases to about 6.843, a touching bifurcation occurs, which means that the standard periodic solution of the Filippov system (8) collides with its tangent point E_2^T. As Y_T continues to increase, the cycle becomes a sliding cycle where sliding occurs on the sliding segment, as shown in Figure 5(c) with $Y_T = 6.9$. When Y_T exceeds 6.98, the virtual equilibrium E_1^V becomes the regular equilibrium E_1^R. In other words, the Filippov system (8) has an unstable regular equilibrium E_2^R and a stable regular equilibrium E_1^R, as shown in Figure 5(d) with $Y_T = 7.2$. At this moment, the sliding cycle remains. In addition, some solution trajectories converge to the stable regular equilibrium E_1^R, as shown by the black curves in Figure 5(d).

Especially when the bifurcation parameter Y_T increases to 8.8, the stable periodic cycle disappears and the regular equilibrium E_2^R becomes the virtual equilibrium E_2^V, as shown in Figure 5(e). Meanwhile, Figure 5(e) also shows that all solution trajectories converge to E_1^R. Figure 5(f) takes the sliding cycle out separately to observe the changes in the sliding cycles. It can be seen from Figure 5(f) that the length of sliding on the slide segment decreases as the sliding bifurcation parameter Y_T increases.

5.4. Impact of k on the System. In this section, we analyze the effect of the fear effect k on the dynamics of the subsystem S_2 and the Filippov system (8). By fixing parameters and initial conditions other than k, we plot the time series diagram of x and y for the subsystem S_2 and the Filippov system (8) for $k = 0, k = 0.3$, and $k = 20$.

It can be seen from Figures 6(a) and 7(a) that the number of predator and prey in the two systems is in a state of periodic fluctuation (i.e. the solution is a periodic solution), but the peak value of fluctuation in Figure 6(a) is higher than that in Figure 7(a). The low-level fear effect ultimately reduce the range of fluctuations in the solutions of the subsystem S_2 and Filippov system (8), and the number of prey is higher than the number of predator, as detailed in Figures 6(b) and 7(b). By observing Figures 6(c) and 7(c), we can see that the quantitative relationship of subsystem S_2 under the high level of fear effect is consistent with that low-level fear effect but finally fluctuates in a smaller range. The high level of fear effect stabilizes the number of predator and prey in the Filippov system (8), but in contrast to the number relationship in the subsystem S_2.

6. Discussion

In recent years, the Filippov system has been widely used in integrated pest management, epidemic control, and predator-prey research [15–18, 21, 30]. The Filippov system demonstrates complex dynamic behaviors on sliding segments based on the inheritance of the dynamic behaviors of atomic systems. New equilibria such as pseudoequilibrium, boundary equilibrium and tangent points can appear on the sliding segment. In addition, new bifurcations such as boundary bifurcations and global sliding bifurcations will also appear on the sliding segment.

In this study, we establish and analyze a Filippov predator-prey model with the fear effect. The threshold of the model is the number of predators, and when the number of predators is below the threshold, the prey does not have a fear effect; when the number of predators exceeds the threshold, the prey has fear effect. Also, the functional responses that respond to the predator-prey relationship are different in the two subsystems.

First, we analyze the existence and stability of the equilibrium of the two subsystems, and discuss whether the equilibria of the two subsystems are regular equilibria or
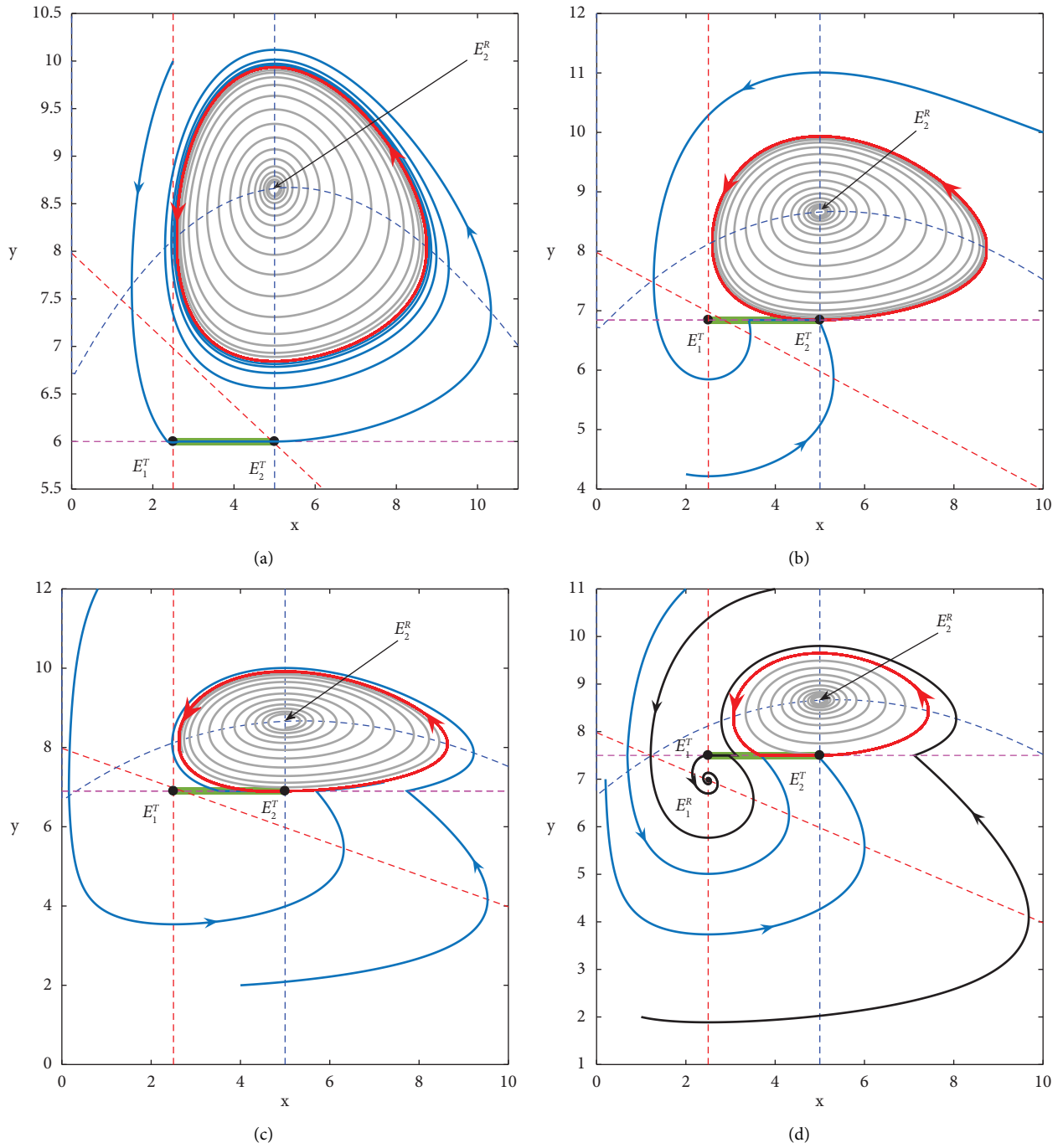
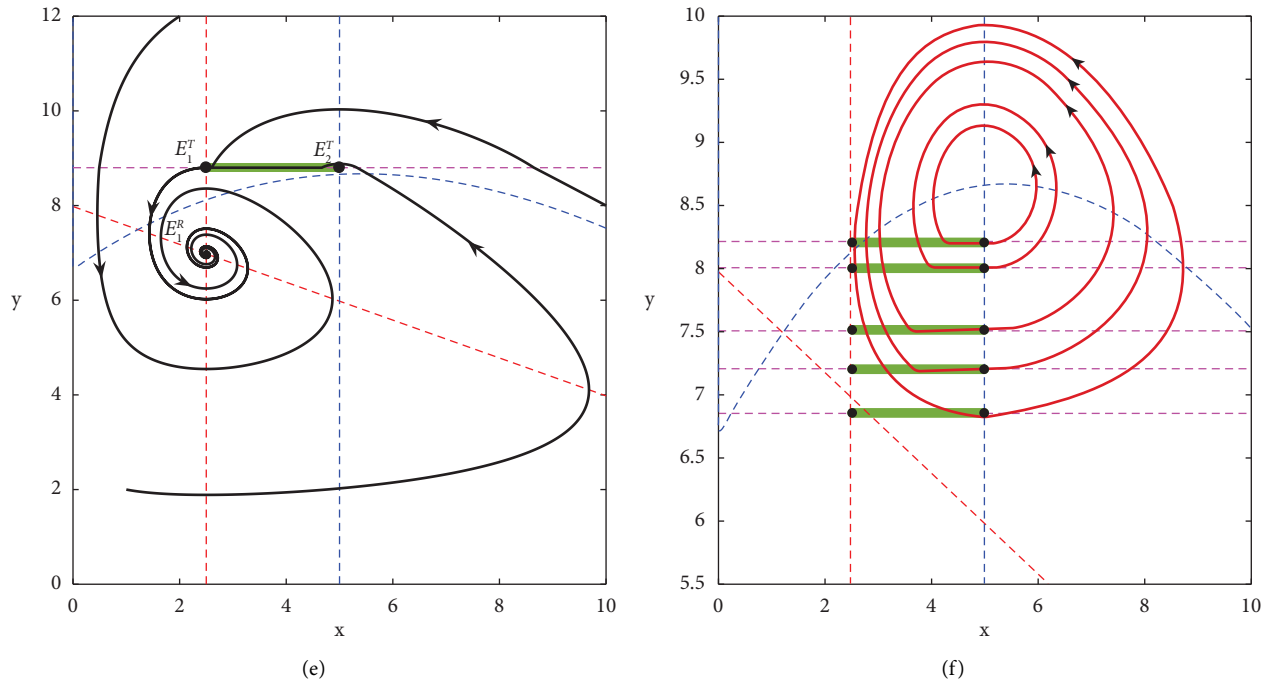(a)

(b)

(c)

(d)

Figure 5: Continued.

(e)

(f)

FIGURE 5: Global sliding bifurcation for system (8). Here, we choose Y_T as a bifurcation parameter and fix all other parameters as follows: $r = 4$, $k = 0.03$, $d = 0.01$, $a = 0.2$, $p = 0.5$, $q = 0.2$, $u = 0.4$, $m = 0.5$, and (a) $Y_T = 6$; (b) $Y_T = 6.843$; (c) $Y_T = 6.9$; (d) $Y_T = 7.2$; (e) $Y_T = 8.8$; and (f) the Y_T values from bottom to top are 6.843, 7.2, 7.5, 8, and 8.2.
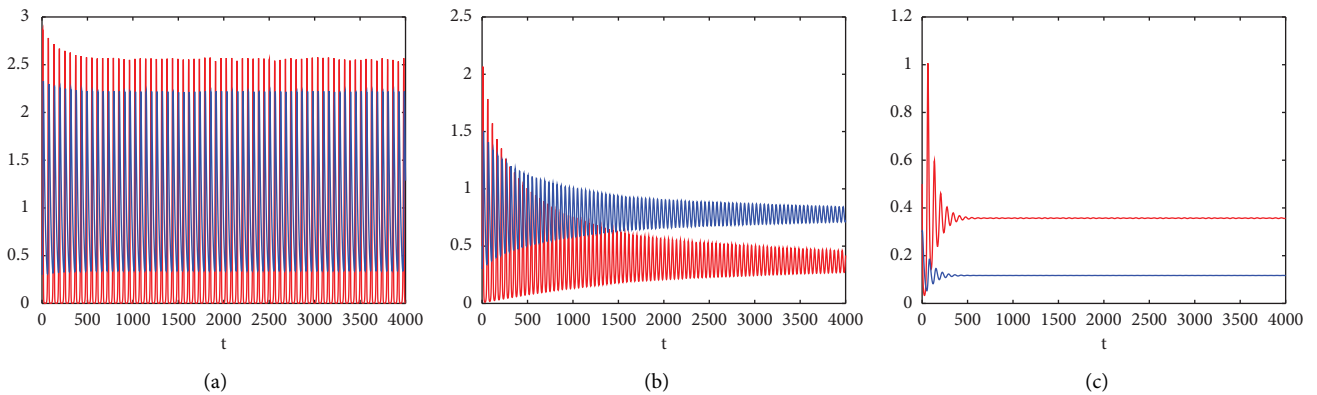

(a)

(b)

(c)

FIGURE 6: Time series diagram of subsystem S_2. Fix the following parameter: $r = 0.6$, $d = 0.1$, $a = 0.07$, $p = 0.5$, $q = 0.2$, $u = 0.3$, $m = 0.05$, and (a) $k = 0$; (b) $k = 0.3$; (c) $k = 20$. The red curve is prey, and the blue curve is predator.

virtual equilibria. The analysis results are summarized in Table 2. In addition, the numerical simulation of the regular/ virtual equilibrium bifurcation is also carried out. It is found that with the change of threshold and birth rate, the regular and virtuality of the equilibria also change, and there will be two regular equilibria or virtual equilibria, as shown in Figure 2. Second, by using the theory of the Filippov system, we give the conditions for the existence of sliding segments and various equilibria. We focus on the existence and stability of the pseudoequilibrium and summarize the results in Table 1.

Finally, we study the boundary equilibrium bifurcation and global sliding bifurcation. From the above numerical

simulation, we find that in the case of $y_1^* > y_2^*$, two virtual equilibria coexist in the system, and a stable pseudoequilibrium appears on the sliding segment. In the case of $y_1^* < y_2^*$, both equilibria of the system are regular equilibria. With the appropriate parameters, the system has a standard periodic solution, as shown in Figure 5(a). With the increase of Y_T, the system exhibits touching bifurcation (Figure 5(b)), sliding cycle (Figure 5(c)), sliding cycle, stable regular equilibrium E_1^R coexistence (Figure 5(d)), and periodic solution disappears (Figure 5(e)).

This paper has obtained some meaningful results, of course, there are some shortcomings. For example, we only analyze the possible existence of pseudoequilibrium using
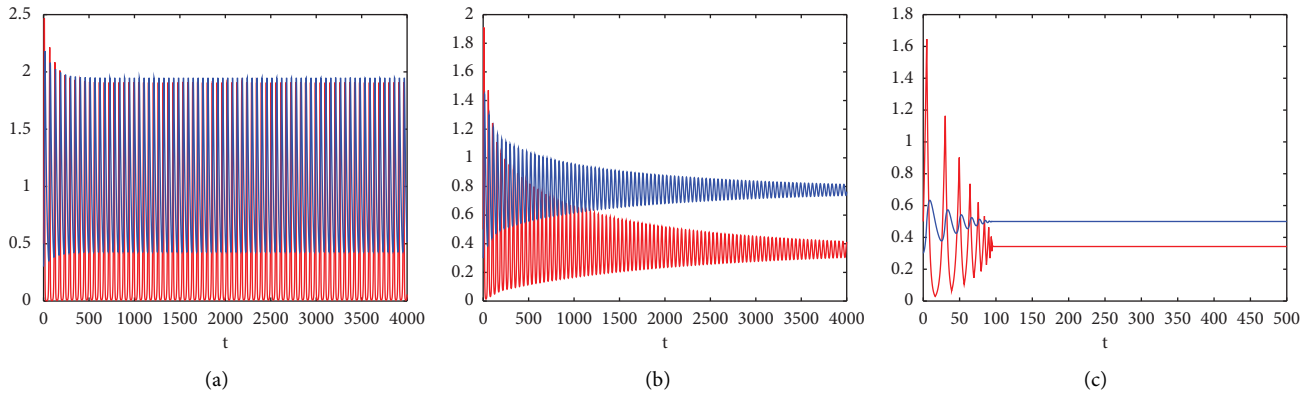
FIGURE 7: Time series diagram of Filippov system (8). Fix the following parameter: $r = 0.6$, $d = 0.1$, $a = 0.07$, $p = 0.5$, $q = 0.2$, $u = 0.3$, $m = 0.05$, $ET = 0.5$, and (a) $k = 0$; (b) $k = 0.3$; (c) $k = 20$. The red curve is prey, and the blue curve is predator.

a combination of theoretical and graphical methods and discuss the local stability of the pseudoequilibrium, without examining their global stability, which will provide a direction for our next study.

Data Availability

The data used to support the findings of this study are included within the article.

Conflicts of Interest

The authors declare that they have no conflicts of interest.

Acknowledgments

References

[1] A. J. Lotka, *Elements of Physical Biology*, Williams & Wilkins, 1925.

[2] V. Volterra, "Fluctuations in the abundance of a species considered mathematically," *Nature*, vol. 118, no. 2972, pp. 558–560, 1926.

[3] S. L. Lima, "Nonlethal effects in the ecology of predator-prey interactions," *BioScience*, vol. 48, no. 1, pp. 25–34, 1998.

[4] S. Creel and D. Christianson, "Relationships between direct predation and risk effects," *Trends in Ecology & Evolution*, vol. 23, no. 4, pp. 194–201, 2008.

[5] W. Cresswell, "Predation in bird populations," *Journal of Ornithology*, vol. 152, no. S1, pp. 251–263, 2011.

[6] X. Wang, L. Zanette, and X. Zou, "Modelling the fear effect in predator–prey interactions," *Journal of Mathematical Biology*, vol. 73, no. 5, pp. 1179–1204, 2016.

[7] J. Wang, Y. H. Chen, L. Lv, and J. Li, "Overlapping group screening for binary cancer classification with TCGA high-dimensional genomic data," *Journal of Bioinformatics and Computational Biology*, vol. 21, no. 3, Article ID 2350013, 2023.

[8] X. Zhang, H. Zhu, and Q. An, "Dynamics analysis of a diffusive predator-prey model with spatial memory and nonlocal fear effect," *Journal of Mathematical Analysis and Applications*, vol. 525, no. 1, Article ID 127123, 2023.

[9] M. Chen, Y. Takeuchi, and J. Zhang, "Dynamic complexity of a modified Leslie–Gower predator–prey system with fear effect," *Communications in Nonlinear Science and Numerical Simulation*, vol. 119, Article ID 107109, 2023.

[10] S. K. Sasmal, "Population dynamics with multiple allee effects induced by fear factors–a mathematical study on prey-predator interactions," *Applied Mathematical Modelling*, vol. 64, pp. 1–14, 2018.

[11] H. Zhang, Y. Cai, S. Fu, and W. Wang, "Impact of the fear effect in a prey-predator model incorporating a prey refuge," *Applied Mathematics and Computation*, vol. 356, pp. 328–337, 2019.

[12] S. K. Sasmal and Y. Takeuchi, "Dynamics of a predator-prey system with fear and group defense," *Journal of Mathematical Analysis and Applications*, vol. 481, no. 1, Article ID 123471, 2020.

[13] B. Chakraborty, H. Baek, and N. Bairagi, "Diffusion-induced regular and chaotic patterns in a ratio-dependent predator–prey model with fear factor and prey refuge, Chaos," *An Interdisciplinary Journal of Nonlinear Science*, vol. 31, no. 3, 2021.

[14] R. Yang and D. Jin, "Dynamics in a predator-prey model with memory effect in predator and fear effect in prey," *Electronic Research Archive*, vol. 30, no. 4, pp. 1322–1339, 2022.

[15] S. Tang, J. Liang, Y. Xiao, and R. A. Cheke, "Sliding bifurcations of Filippov two stage pest control models with economic thresholds," *SIAM Journal on Applied Mathematics*, vol. 72, no. 4, pp. 1061–1080, 2012.

[16] W. Qin, X. Tan, M. Tosato, and X. Liu, "Threshold control strategy for a non-smooth Filippov ecosystem with group defense," *Applied Mathematics and Computation*, vol. 362, Article ID 124532, 2019.

[17] W. Li, Y. Chen, L. Huang, and J. Wang, "Global dynamics of a Filippov predator-prey model with two thresholds for integrated pest management," *Chaos, Solitons & Fractals*, vol. 157, Article ID 111881, 2022.

[18] W. Li, L. Huang, and J. Wang, "Global asymptotical stability and sliding bifurcation analysis of a general Filippov-type predator-prey model with a refuge," *Applied Mathematics and Computation*, vol. 405, Article ID 126263, 2021.

[19] J. Wang, F. Zhang, and L. Wang, "Equilibrium, pseudoequilibrium and sliding-mode heteroclinic orbit in a Filippov-

type plant disease model," *Nonlinear Analysis: Real World Applications*, vol. 31, pp. 308–324, 2016.

[20] C. Chen, Y. Kang, and R. Smith, "Sliding motion and global dynamics of a Filippov fire-blight model with economic thresholds," *Nonlinear Analysis: Real World Applications*, vol. 39, pp. 492–519, 2018.

[21] S. Tang, Y. Tian, and R. A. Cheke, "Dynamic complexity of a predator-prey model for ipm with nonlinear impulsive control incorporating a regulatory factor for predator releases," *Mathematical Modelling and Analysis*, vol. 24, no. 1, pp. 134–154, 2019.

[22] M. Biák, T. Hanus, and D. Janovská, "Some applications of Filippov's dynamical systems," *Journal of Computational and Applied Mathematics*, vol. 254, pp. 132–143, 2013.

[23] Y. V. Tyutyunov and L. Titova, "From lotka–volterra to arditi–ginzburg: 90 years of evolving trophic functions," *Biology Bulletin Reviews*, vol. 10, no. 3, pp. 167–185, 2020.

[24] J. Yang, S. Tang, and R. A. Cheke, "Global stability and sliding bifurcations of a non-smooth Gause predator–prey system," *Applied Mathematics and Computation*, vol. 224, pp. 9–20, 2013.

[25] X. Zhang and S. Tang, "Existence of multiple sliding segments and bifurcation analysis of Filippov prey–predator model," *Applied Mathematics and Computation*, vol. 239, pp. 265–284, 2014.

[26] X. Zhang and S. Tang, "Filippov ratio-dependent prey-predator model with threshold policy control," *Abstract and Applied Analysis*, vol. 2013, Article ID 280945, 11 pages, 2013.

[27] R. Cristiano, T. Carvalho, D. J. Tonon, and D. J. Pagano, "Hopf and homoclinic bifurcations on the sliding vector field of switching systems in R3: a case study in power electronics," *Physica D: Nonlinear Phenomena*, vol. 347, pp. 12–20, 2017.

[28] B. Tang and W. Zhao, "Sliding dynamics and bifurcations of a Filippov system with nonlinear threshold control," *International Journal of Bifurcation and Chaos*, vol. 31, no. 14, Article ID 2150214, 2021.

[29] Y. A. Kuznetsov, S. Rinaldi, and A. Gragnani, "One-parameter bifurcations in planar Filippov systems," *International Journal of Bifurcation and Chaos*, vol. 13, no. 08, pp. 2157–2188, 2003.

[30] A. Wang and Y. Xiao, "Sliding bifurcation and global dynamics of a Filippov epidemic model with vaccination," *International Journal of Bifurcation and Chaos*, vol. 23, no. 8, Article ID 1350144, 2013.